Laser-aided manufacturing of ultra-high-aspect ratio optical fibers

P. Maniewski[a,b], Bruno Moog[b], Matthew Whitaker[b], Christopher Holmes[b]

[a] Department of Applied Physics, KTH Royal Institute of Technology, Stockholm, Sweden
[b] Optoelectronic Research Centre, University of Southampton, Southampton, United Kingdom

ABSTRACT

The current landscape of optical fiber technology is dominated by fibers with a circular cross-section with axial symmetry and a centrally positioned waveguiding core. This typical layout is dictated by traditional manufacturing routes that often utilize furnaces, gas burners, and glass lathes. Contrastingly, in our work, we utilize laser-based glass additive-manufacturing to melt, weld, and reshape glass powders and prefabricates to create fiber preforms. Additionally, through a combination of mid-IR CO_2 laser melting and oxide nano-powder jets aimed into laser-induced hot-zone, high quality glass features can be 3D-printed onto the fiber preform. In our work we focus on high-aspect ratio preforms that can be then drawn in traditional draw towers into over 100 m long ultra-thin fibers. Here, flat fibers as thin as 35 µm and aspect-ratio of up to 27:1 with sub-µm surface flatness were made. Furthermore, by utilizing this novel print-stack-draw approach, microstructure and chemically doped features for e.g., waveguiding and optical gain can be spatially tailored, both laterally and along the direction of draw. Compatibility of these fibers with standard counterparts such as commercial single-mode-fibers was demonstrated through e.g., laser-based splicing. The new manufacturing approach utilized in this work unlocks highly flexible, novel photonic designs with large disruptive potential for areas including lab-in-fiber, physical sensors and fiber lasers.

Keywords: optical fiber, laser manufacturing, flat fiber, glass 3d printing

1. INTRODUCTION

Specialty fiber optics are arguably at the frontiers of modern technology, serving as catalysts for innovation in communications, sensing, and medical applications. Fiberized devices for physical and chemical sensing, inertial navigation, light amplification and lasers, offer significant advantages due to their inherent compact design, material efficiency, and manufacturing scalability. Unlike traditional bulk optics or discrete components, fiberized devices integrate various optical elements directly into the fiber, minimizing the need for additional housing, alignment, and packaging. This integration not only reduces the costs associated with traditional manufacturing but also streamlines the assembly process, leading to lower labor costs and faster production times. This reduces the barrier to entry for new applications and technologies, making fiberized devices a cost-efficient choice for both large-scale deployments and specialized applications.

For optical fiber production, homogeneous, ultra-high-purity materials are essential to achieve ultra-low transmission losses and high-performance glass. These materials are used to fabricate fiber preforms, which are typically produced by assembling vapor-deposition-derived rods and tubes. The preforms are scaled up into assemblies that resemble the structure of the desired fiber. These preforms are then drawn into fibers with the required dimensions. Consequently, industrial standard fiber typically features a round cross-section with a diameter of 125 µm when drawn, with a centrally located waveguiding core. Larger-diameter fibers, often employed in high-power applications to reduce nonlinear effects and increase damage thresholds, generally exhibit reduced mechanical flexibility, while more flexible smaller-diameter fibers are advantageous particularly in the case of embedded structural monitoring of glass or carbon fiber reinforced polymer (GFRP/CFRP), that is commonly used in high-value automotive and aerospace components, wind turbine blades etc. [1]. For monitoring of CFRP, the sensors are typically laid in-between structural-fiber plies during lay-up.

On the contrary to traditional fiber preform manufacturing that is based on vapor-deposition techniques, laser-based fabrication techniques demonstrate certain advantages including non-contact interaction, rapid processing and spatially localized heating [2–5]. For silica glass, a confined CO_2 laser-induced hot zone enables thermal regime that is suitable for a broad range of glass manufacturing capabilities. At the typical wavelengths of CO_2 lasers ($\lambda = 10.6$ µm) silica is highly absorbing, with a typical penetration depth of just a few microns. Absorption of the beam leads to rapid temperature increase upon exposure. During CO_2 laser processing, heating and cooling rates can be extremely high,

exceeding 10 000 K/s, with broad tunability. Such thermodynamics can be leveraged to cut, weld, polish or reshape silica components [3,6–9]. Furthermore, in our work, we utilize laser powder deposition (LPD) for additive manufacturing of high-quality silica glass [10,11]. Here by combination of a CO_2 laser beam and a powder jet, a high-quality silica glass featuring the desired doping can be printed at the desired locations of a substrate. In the realm of specialty active fibers, LPD enables e.g., relatively low-transmission loss and high gain [12].

In this work, we leverage this unconventional manufacturing approach to fabricate new preform architectures that would be challenging to obtain otherwise. Subsequently, the preforms are drawn using a traditional fiber drawing tower. Specifically, in this work, we target exploration of ultra-high aspect ratio flat optical fiber (FF) for embedded sensing. Such fibers show several advantages over their round counterparts. Flat fibers with a high aspect ratio of up to 27:1, with a width of over 1.7 mm, and a thickness down to approximately 35 µm ensures easy manual handling and alignment of such fiber, as well as minimal interference with the surrounding material during sensor integration. By utilizing LPD, chemically doped features, i.e., multi-core fibers were made, with each core located at the strategically designed positions.

2. FABRICATION OF ULTRA-HIGH ASPECT RATIO FIBER

For preform preparation we developed a 60W CO_2 laser-equipped system similar to the one described in detail in [11]. Generally, fiber fabrication consisted of 3 steps as depicted in Fig. 1. First, a planar silica glass substrate was laser-cut to the desired dimensions. Subsequently, chemically doped features were printed onto it. For example, to obtain the waveguides, we used an alumina-silica powder mixture; silica was used as the host, while alumina was used to increase refractive index of the printed glass, thus providing waveguiding conditions [2]. The mixture was fed via a single off-axis powder jet, aimed at a laser-induced hot-zone. Subsequently, by scanning the substrate using a pre-defined path (speed of 6 mm/s), a fully sintered 'ridge' was fabricated. The extended versality of our manufacturing system enabled also laser-welding of prefabricated preform components, e.g., the tube handles that enable to mount and draw the high AR preform in a typical draw-tower normally used for round fibers. The typical fully assembled preform was 1 m long (including the tubes), 33 mm wide and 1-3 mm thick.

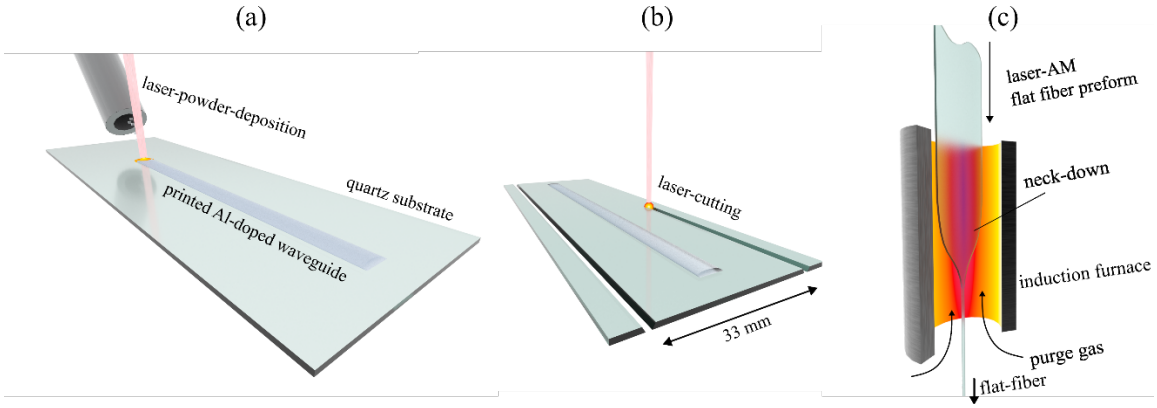

Figure 1 Sketch of main fabrication steps of high AR fiber: (a) laser-powder-deposition of waveguides (see Ref [11]), (b) cutting and pre-shaping, (c) fiber drawing.

The assembled preform was drawn into a fiber using a traditional fiber draw tower equipped with an induction furnace. The furnace, with a diameter of 35 mm, limited the maximum width of our preforms. The preform was inserted into the furnace from the top and positioned as required. As it heated, the softened glass elongated due to the combined effects of gravity and viscosity, forming a drip. This drip remained connected to the preform by a thin fiber in the neck-down region, where the preform was translated to obtain the desired fiber dimensions.

Unlike their round counterparts, the drawing of FFs exhibited non-homothetic drawing. To gain a deeper understanding of neck-down formation and FF drawing behavior, we drew a few identical preforms under varying speeds and temperatures. In all experiments, the preform feeding speed was maintained at a constant 1 mm/min. Figure 2 illustrates the width and thickness of the FF as functions of the drawing conditions.

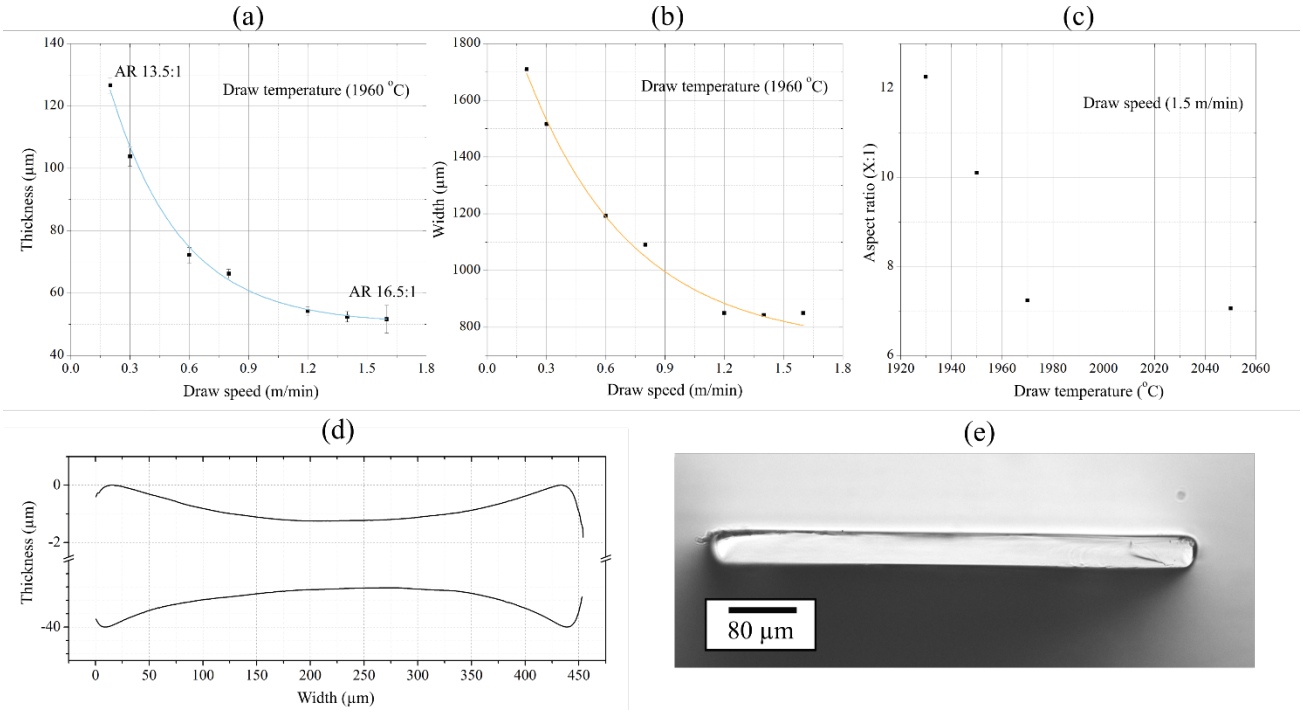

Figure 2 Flat fiber thickness (a), width (b), and aspect ratio (c) for different drawing parameters. Profilometry (d) of top and bottom surface of a proof-of-concept FF drawn at 1950°C and (e) the typical cross-section of high AR FF.

3. CONCLUSION

By leveraging CO_2 laser-assisted manufacturing we fabricated preforms and then drew an ultra-high aspect ratio fiber. A single preform was drawn into over 100 m of continuous fiber using a traditional drawing tower equipped with an induction furnace. During drawing, the preform showed inhomogeneous necking i.e., in the neck down region the width of the preform was reduced significantly more than its thickness. Such dynamics can be linked to temperature gradient in the furnace. Thereby this drawing dynamics should be accounted for in preform design to obtain the desired high-aspect-ratio cross section of the drawn fiber. The width and thickness of the resultant fiber can be linked to the ratio between preform feeding rate and drawing speed and change of the draw speed had a minor impact on the resultant aspect ratio. However, the aspect ratio could be largely tuned by changing the draw temperature. Higher drawing temperature resulted in lower aspect ratio of the fiber, and this can be linked to viscous forces of softened glass in the neck down region. For example, in our experiments we fabricated over 100 m of a continuous ultra-high aspect ratio fiber that was 37 µm thin, with the width of 560 µm. It was drawn at 1950°C with the drawing speed up to 1.5 m/min. The surface profile showed variance not larger than 1 µm in its center. The high flatness and low thickness of the fiber show promising results towards future integration of flat-fiber-based sensors with fiber-reinforced polymers.

ACKNOWLEDGEMENTS

This work is supported by Swedish Research Council (VR) (2022-06180); Stiftelsen Tornspiran (894, 1027); Engineering and Physical Sciences Research council (EP/Y016920/1).

REFERENCES

1. C. Holmes, M. Godfrey, P. L. Mennea, S. Zahertar, and J. M. Dulieu-Barton, "Flexible photonics in low stiffness doped silica for use in fibre reinforced polymer composite materials," Opt Mater (Amst) **134**, 113133 (2022).

2. P. Maniewski, T. J. Wörmann, V. Pasiskevicius, C. Holmes, J. C. Gates, and F. Laurell, "Advances in laser-based manufacturing techniques for specialty optical fiber," Journal of the American Ceramic Society **107**, 5143–5158 (2024).
3. V. K. Sysoev, B. N. Planida, A. A. Verlan, P. A. Vyatlev, M. A. Pomerantsev, T. A. Aliev, and B. P. Papchenko, "Laser welding of quartz glass workpieces," Glass and Ceramics **68**, 389–392 (2012).
4. L. Pohl, P. von Witzendorff, E. Chatzizyrli, O. Suttmann, and L. Overmeyer, "CO2 laser welding of glass: numerical simulation and experimental study," The International Journal of Advanced Manufacturing Technology **90**, 397–403 (2017).
5. J. Luo, L. J. Gilbert, C. Qu, R. G. Landers, D. A. Bristow, and E. C. Kinzel, "Additive Manufacturing of Transparent Soda-Lime Glass Using a Filament-Fed Process," J Manuf Sci Eng **139**, (2017).
6. L. Brusberg, M. Queisser, C. Gentsch, H. Schröder, and K.-D. Lang, "Advances in CO2-Laser Drilling of Glass Substrates," Phys Procedia **39**, 548–555 (2012).
7. A. Heptonstall, M. A. Barton, A. Bell, G. Cagnoli, C. A. Cantley, D. R. M. Crooks, A. Cumming, A. Grant, G. D. Hammond, G. M. Harry, J. Hough, R. Jones, D. Kelley, R. Kumar, I. W. Martin, N. A. Robertson, S. Rowan, K. A. Strain, K. Tokmakov, and M. van Veggel, "CO2 laser production of fused silica fibers for use in interferometric gravitational wave detector mirror suspensions," Review of Scientific Instruments **82**, (2011).
8. C. Weingarten, E. Uluz, A. Schmickler, K. Braun, E. Willenborg, A. Temmler, and S. Heidrich, "Glass processing with pulsed CO_2 laser radiation," Appl Opt **56**, 777 (2017).
9. E. Mendez, K. M. Nowak, H. J. Baker, F. J. Villarreal, and D. R. Hall, "Localized CO2 laser damage repair of fused silica optics," Appl Opt **45**, 5358 (2006).
10. P. Maniewski, F. Laurell, and M. Fokine, "Quill-free additive manufacturing of fused silica glass," Opt Mater Express **12**, 1480–1490 (2022).
11. P. Maniewski, F. Laurell, and M. Fokine, "Laser cladding of transparent fused silica glass using sub-µm powder," Opt Mater Express **11**, 3056–3070 (2021).
12. P. Maniewski, M. Brunzell, L. Barrett, C. Harvey, V. Pasiskevicius, and F. Laurell, "Er-doped silica fiber laser made by powder-based additive manufacturing," Optica **10**, 1280–1286 (2023).